Link to published version https://doi.org/10.1016/j.dyepig.2020.108401

# Structural order and NIR reflective properties of perylene bisimide pigments: experimental evidences from a combined multi-technique study

*Francesca Martini,[1,2,3,‡] Pierpaolo Minei,[1,‡] Marco Lessi,[1] Luca Contiero,[4] Silvia Borsacchi,[2,5] Giacomo Ruggeri,[1,2] Marco Geppi,[1,2,3] Fabio Bellina,[1,2,3] Andrea Pucci[1,2,3,*]*

[1]Dipartimento di Chimica e Chimica Industriale, Università di Pisa, Via Giuseppe Moruzzi 13, 56124 Pisa, Italy
[2]INSTM, UdR Pisa, Via Giuseppe Moruzzi 13, 56124 Pisa, Italy
[3]CISUP, Centro per l'Integrazione della Strumentazione dell'Università di Pisa, Lungarno Pacinotti 43, Pisa
[4]Cromology Italia S.P.A. Via 4 Novembre 4, 55016 Porcari, Lucca, Italy
[5]Istituto di Chimica dei Composti Organo Metallici (ICCOM), Consiglio Nazionale delle Ricerche, SS Pisa, Via G. Moruzzi 1, 56124 Pisa, Italy
‡These authors contributed equally

Corresponding author:

Prof. Andrea Pucci, Dipartimento di Chimica e Chimica Industriale, Università di Pisa, Via Giuseppe Moruzzi 13, 56124 Pisa, Italy. Email: *andrea.pucci@unipi.it*

**Keywords:** perylene bis-imides pigments, crystallinity, organic coatings, NIR reflectivity, cooling effect

**Abstract**

This study reports the effect of the crystallinity degree and structural order of the supramolecular architectures of the perylene derivative Paliogen® Black L0086 (P-black) on the near-infrared (NIR) transparent, reflective and cooling characteristics of 75 μm thick acrylic coatings. Notably, XRD and solid-state NMR investigations revealed that on passing from the commercially available P-black C to the synthetic form P-black S, the average crystallinity passed from 20 to 48% flanked by a superior structural order that enhanced the mean crystallite width from 21.7 to 39.1 nm and maximum length from 1.5 μm to 6.5 μm, as evidenced by SEM micrographs. UV-VIS-NIR spectroscopic analyses of the coated surfaces confirmed the NIR transparent and reflective characteristics of the P-black pigment that was particularly relevant in the case of the pigment synthetic form. NIR reflectance enhancements from 25% to 50% were actually recorded on black surfaces on passing from the commercial to the synthetic form of the pigment dispersed into the acrylic coatings. This feature was reflected on the solar reflectance and the cooling effect, with values boosted from 9.9% to 18.2% and from 2.3 °C to 3.8 °C, respectively.

## 1. Introduction

Perylene bis-imide derivatives (PBIs) represent an important class of pigments, dyes and fluorophores, with colors ranging from red to black depending on molecular packing among the chromophoric units.[1-4] PBIs display strong absorption in the visible region, excellent photostability and high fluorescence quantum yields when functionalized with moieties able to prevent the aggregation-caused quenching (ACQ) phenomenon.[5-12] PBIs also display a low reduction potential that enables their use as semiconductors in photoinduced charge-transfer reactions. For these appealing features, PBIs have been the object of considerable interest for the production of field-effect transistors,[13-15] luminescent solar concentrators for photovoltaic cells,[16-22] organic light-emitting diodes (OLEDs)[23] and chromogenic additives for smart and intelligent polymers.[8, 9, 24-28]

Also, in recent years, there has been a growing interest in the application of PBIs as photo- and thermo-stable *cool* organic pigments since they are reported to display Near-Infrared (NIR) transparency and reflectivity.[29-32] Coatings based on *cool* pigments are proposed as accessible solutions to mitigate the warming effect provided by the sunlight exposure, thus resulting beneficial for downgrading the urban heat island effect.[33-38] Notably, organic coatings based on NIR-reflective PBIs are reported to show about 40% of NIR reflectance and cooling effects of the coated black surfaces of more than 10 °C. All these features appear to be attributed to the high-symmetry PBI conformation characterized by a zero dipole moment, which tends to generate crystalline supramolecular assemblies thanks to the intermolecular π-π interactions among perylene chromophores.[30, 32, 39-41]

Recently, Paliogen® Black L0086 (P-black, Figure 1) has been proposed in combination with thermoplastic hollow microspheres (THM) to increase the NIR reflecting characteristics of the organic coating.[29] P-black is a black PBI distributed by BASF as pigment for solar heat management in paints.[42] Notwithstanding the low crystalline content of the P-black pigment (i.e., about 20%), coatings

based of mixtures between P-black and THM provided maximum NIR reflectances of more than 45% and solar reflectance (SR) of 22.

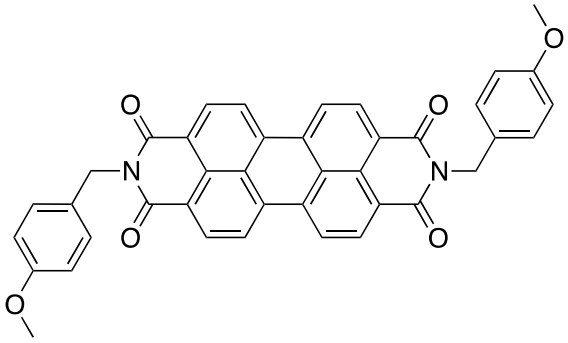


Figure 1. Chemical structure of Paliogen® Black L0086 (P-black)

In connection with these findings, in this work, we investigated the influence of the crystalline content and the structural disorder of the P-black pigment on its NIR transparent and reflective properties when physically dispersed in organic acrylic coatings. Notably, two different types of P-black were utilized: a commercially available source provided by BASF (i.e., P-black C) and a synthetic derivative (i.e., P-black S) that are characterized by different crystallinity degree. XRD and ssNMR investigations were utilized to determine the structural characteristics of both forms of P-black and the results discussed in terms of the different cooling effect determined by solar reflectance and temperature measurements.

## 2. Experimental part

*Materials*

3,4:9,10-Perylenebis anhydride, $Zn(OAc)_2 \cdot 2H_2O$, imidazole and 4-methoxybenzylamine were purchased from Sigma-Aldrich and utilized as received. Disperbyk 2015 was obtained from BYK USA Inc. PRIMAL™ E-822K (Acrylic dispersion polymer, 50% solid content, $T_g$ = 18 °C) was supplied by the Dow Chemical Company. The commercially available pigment P-black (P-black C) was provided by BASF (Paliogen® Black L0086) and used without further purification.

*Synthesis of N,N'-Bis-(4-methoxybenzyl)-3,4:9,10-perylenetetracarboxybis-imide (P-black S)*

P-black S were prepared according to a slightly modified procedure described by BASF.[43] Perylene-3,4:9,10-tetracarboxylic acid bisanhydride (0.39 g, 1.0 mmol), $Zn(OAc)_2 \cdot 2H_2O$ (0.22 g, 1.00 mmol), and imidazole (7.85 g, 115 mmol) were placed in a reaction vessel under a stream of argon. The reaction vessel was fitted with a silicon septum, evacuated and back-filled with argon, and this sequence was repeated three times. Deareated 4-methoxybenzylamine (0.33 mL, 0.32 g, 2.50 mmol) was then added by syringe under a stream of argon, and the resulting mixture was stirred at 160 °C for 21 h. After this period, the reaction mixture was cooled to 90 °C and diluted with MeOH (20 mL). The resulting suspension was stirred for 15 min, then cooled to room temperature and filtered. The filter cake was washed with MeOH (3 x 10 mL), 5% $HCl_{aq}$ (3 x 10 mL), with pure water until neutrality (4 x 10 mL), and oven-dried at 105 °C overnight to give the required perylene bisimide (0.60 g, 96%) as a black solid: mp > 300 °C (decomp.). $^1$H NMR (400 MHz, $D_2SO_4$) $\delta$ 9.53 (m, 12H), 8.45 (m, 4H), 6.08 (s, 4H), 4.41 (s, 6H). IR ($cm^{-1}$): 1691, 1659, 1591, 1514, 1257. $C_{40}H_{26}N_2O_6$ (630.66): calcd. C 76.18, H 4.16, N 4.44; found C 76.54, H 4.12, N 4.40.

*Coating preparation*

The organic coatings were prepared according to the literature.[29, 40] Briefly, 2 g of the acrylic PRIMAL™ E-822K resin were combined at room temperature to a desired amount of P-black and

Disperbyk 2015 (1:1 by weight), and the mixture was gently mixed to obtain a homogeneous dispersion. Then, 500 μL of deionized $H_2O$ were added and the resultant dispersion was coated on Leneta® checkerboard charts by using the universal applicator ZUA 2000 (Zehntner Testing Instruments). P-black coating films were obtained after drying at room temperature under a hood with a thickness of 75 μm (CM1S dial indicator, Borletti, Milan, Italy).

*Methods*

Infrared spectra were performed with a Fourier transform spectrometer PerkinElmer™ Spectrum 100 on KBr dispersions. $^1$H-NMR spectrum of P-Black S was recorded at room temperature in $D_2SO_4$ solution with a Bruker Avance DRX 400 spectrometer, using the residual solvent peak as internal reference; chemical shifts ($\delta$) values are given in parts per million (ppm). Elemental analyses were performed on a Elementar Vario Micro Cube CHN-analyzer.

$^{13}$C high-resolution ssNMR spectra were recorded on a Varian InfinityPlus 400 spectrometer, equipped with a 3.2 mm Cross-Polarization/Magic Angle Spinning (CP/MAS) probehead, for rotors with inner diameter of 3.2 mm. The Larmor frequencies were 400.35 and 100.67 MHz for $^1$H and $^{13}$C nuclei, respectively, with 90° pulse durations of 1.8 μs ($^1$H) and 2.7 μs ($^{13}$C). The MAS frequency was always set at 15 kHz, and a SPINAL pulse scheme was used for $^1$H-$^{13}$C high-power decoupling, with a decoupling field of 87 kHz. For the $^{13}$C CP/MAS spectra a linear ramp of the $^{13}$C cross-polarization field was applied during CP, using a contact time (*ct*) of 2 ms. The spectra were obtained accumulating 6000-12000 transients, waiting a recycle delay between consecutive scans (*rd*) of 5 s. $^{13}$C Direct Excitation (DE) spectra were acquired accumulating 16000 transients with a *rd* of 2 s. All the experiments were carried out at room temperature using air as spinning gas. Tetramethyl silane and hexamethylbenzene were taken as primary and secondary references, respectively, for the $^{13}$C chemical shift scale. X-ray powder diffraction (XRD) was performed according to the literature[44] and using a Bruker D2 Phaser diffractometer operating in Bragg-Brentano geometry and equipped with a 1-dimensional Lynxeye

detector. Scanning electron microscopy (SEM) was performed using a FEI Quanta 450 ESEM equipped with a field emission gun. The powders were deposited without grinding over graphite supports and a few nm of Pt were then sputtered on their surfaces. UV–Vis–NIR reflectance measurements of black and white coated surfaces were recorded over the wavelength range of 300–2500 nm by using an Agilent Cary 5000 spectrophotometer equipped with a 150 mm integration sphere and according to ASTM E903-12 (Standard Test Method for Solar Absorptance, Reflectance, and Transmittance of Materials Using Integrating Spheres). NIST standards were utilized as primary standards for the calibration of instrument. The solar reflectance (SR) index was computed by integrating the measured spectral data weighted with the air mass 1.5 beam-hemispherical solar spectral irradiance for 37° sun-facing tilted surface, as described in ASTM G173-03. A solar simulator (ORIELs LCS-100 solar simulator 94011A S/N: 322, AM 1.5G std filter: 69 mW $cm^{-2}$ at 254 mm) was housed 30 cm above the uncoated and coated black side of Leneta® checkerboard chart. The temperature of the back side of the Leneta® checkerboard chart was recorded by a wire K-type thermocouple probe connected to a MITEK MK 5303 thermometer with a resolution of 0.1 °C. The temperature of the room was maintained constant during the measurements in order to avoid the heating of the sample by convection of the air.

## 3. Results and discussion

*X-ray powder diffraction (XRD)*

The X-ray diffractograms of the synthetic P-black S and the commercial P-black C pigments are reported in Figure 2.

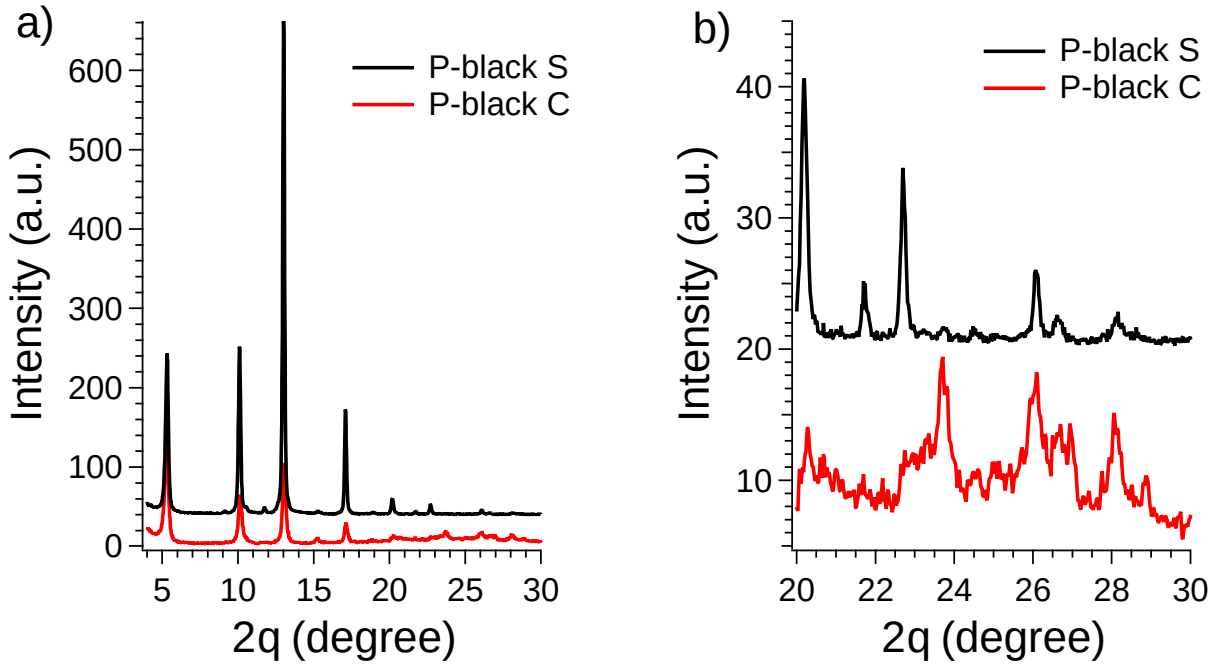


Figure 2. a) XRD spectra of P-black S (black curve) and P-black C (red curve) and b) magnification of the peak reflections in the high theta region (2θ = 20-30°).

P-black S shows intense and sharp peaks associated to the crystalline phase of P-black,[29] with negligible baseline deviations that are typically attributed to the amorphous content of the pigment. P-black C displays the same XRD pattern of P-black S but with less intense contributions and accompanied by the presence of broad reflections at high 2θ angles (20-28°) that are typically attributed to a certain degree of local disorder in the molecular packing of the PBI chromophores.[10]

The crystallinity degrees of both P-black pigments were then calculated from their XRD patterns in agreement with equation 1:

$$\text{crystallinity degree} = \frac{I_c}{I_c + I_a} \qquad \text{(Eq. 1)}$$

where $I_c$ is the area under the sharp peaks and is referred to the scattering intensity from the crystalline content, whereas $I_a$ is the related amorphous contribution. The calculated crystallinity degree of P-black C was about 20% and agrees well with that reported recently by us.[29] Conversely, the degree of crystallinity of P-black S was calculated to be about 48%, i.e. more than two times higher than that evaluated from the commercial pigment source. Moreover, the full width at half maximum ($\Delta(2\Theta)$) calculated for the peak centred at $2\Theta = 5°$ changes from 0.3658° to 0.2032° on passing from P-black C to P-black S. Application of Scherrer's equation[45] $0.9 \cdot \lambda / \Delta(2\Theta) \cdot \cos\Theta$ evidenced a striking increase of the mean crystallite size from 21.7 to 39.1 nm, respectively. These findings suggest that the synthetic and the purification approach carried out during the preparation of P-black S have favored the formation of more regular and compact supramolecular assemblies of the PBI pigment.

*Solid State NMR*

In our recent publication [29] we reported for the first time the $^{13}C$ CP/MAS high-resolution spectrum of P-black C. In Figure 3a, this spectrum is compared with that recorded in the same experimental conditions for P-black S. The spectra are very similar and show the main carbon signals of the perylene bisimide core and of the methoxybenzyl side groups. As already observed [29], the full spectral assignment of the aromatic spectral region is not straightforward, due to the complex overlapping of a multiplicity of signals, which is explainable with the symmetry of the local supramolecular packing or molecular conformation rather than with the chemical structure. A remarkable difference between the two spectra regards the signal at about 114 ppm, which is clearly observable in the spectrum of P-black C, while it cannot be detected in the spectrum of P-black S (see also the expansion of the relevant spectral region in Figure S1). It is worth noting that the chemical shift of this signal is exactly the mean of those at 111 and 117 ppm, which can be reasonably ascribed to carbon atoms 16/16a and 18/18a (from now on carbons n/na will be indicated as n(a) for the sake of simplicity) belonging to the same methoxybenzyl group, but

experiencing slightly different structural environments due to a blocked molecular conformation. In contrast, the signal at 114 ppm is attributable to a fraction of molecules, for which there is a fast exchange between carbons 16(a) and 18(a). This could be either due to the presence of motions such as the π-flips of the phenyl ring[46] or of the methoxyl group, with a characteristic frequency (inverse of the correlation time of the motion) much higher than the difference in frequency between the two carbon signals (600 Hz). This assignment is further supported by the $^{13}C$ DE/MAS spectra shown in Figure 3b. These spectra were recorded with a short recycle delay of 2 s to enhance the signals of carbons in mobile environments, typically characterized by short $T_1$ values. In these spectra the most intense signal is that of the methoxyl group, due the fast rotation of the methyl group around its ternary symmetry axis.[47] Noticeably, in the aromatic region the spectrum of the P-black C contains only the peak at 114 ppm and a signal of comparable intensity at 131 ppm, which is ascribable to carbons 15(a) and 19(a). Both signals should arise from a fraction of molecules with the phenyl rings undergoing a fast π-flip motion in the MHz frequency regime: indeed, only such a motion could be effective in shortening the $T_1$'s of all the ternary carbons of the phenyl ring, through the modulation of their $^{1}H$-$^{13}C$ dipolar interactions. Accordingly, these signals are expected to be depressed in the CP spectrum with respect to those ascribable to the same carbons in a rigid environment.[48] This motion could be present in molecules located in a disordered environment, as, for example, those in proximity to the edges of the crystal structures, where less compact and ordered stacked aggregates are probably formed. It is interesting to notice that, in agreement with $^{13}C$ CP/MAS spectra, practically no signal is detectable in the aromatic spectral region of the $^{13}C$ DE/MAS spectra of P-black S (Figure 3b), suggesting that the amount of structural defects in this sample is negligible. This result has a good correspondence with the XRD results, according to which for P-black S the degree of crystallinity is higher and the crystallites are characterized by larger dimensions than in P-black C, so that the "edges effects" could become barely detectable.

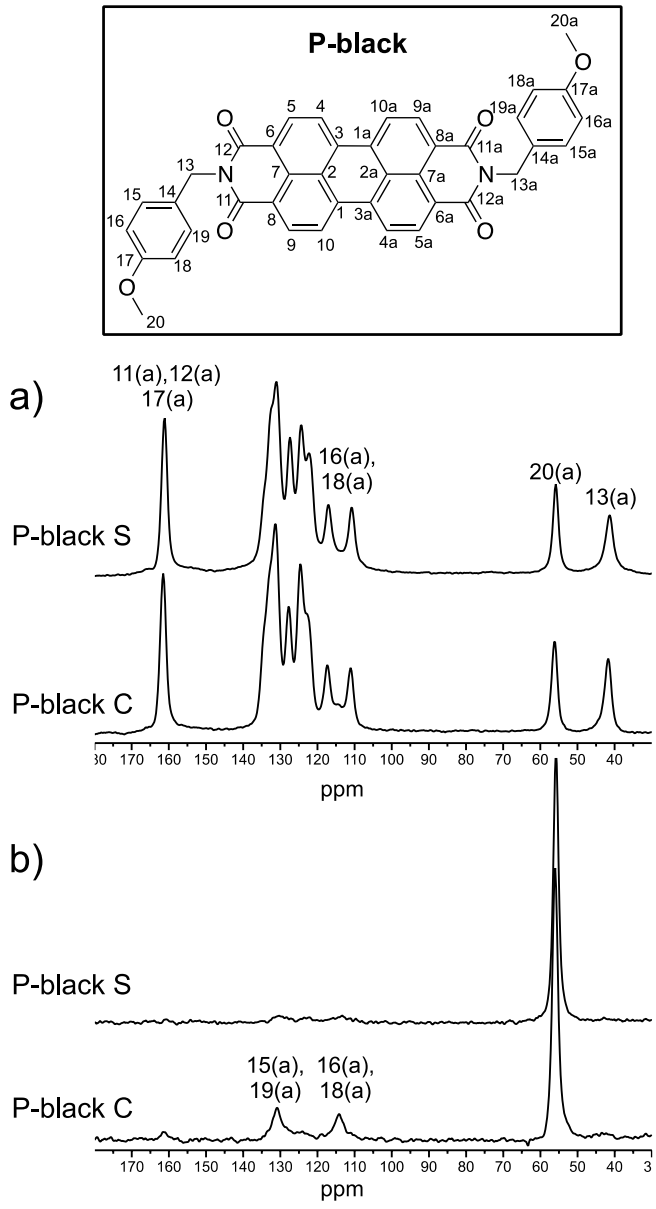


**Figure 3.** a) $^{13}C$ CP/MAS spectra and b) $^{13}C$ DE/MAS spectra recorded with a *rd* of 2 s of P-black C and P-black S. It should be noted that in ref. 29 carbons 15 and 19 were erroneously indicated in the place of carbons 16 and 18 for the signals between 111 and 117 ppm.

*Scanning Electron Microscopy (SEM)*

SEM micrographs taken on P-black C (Figure 4a) and P-black S (Figure 4b) pigments showed different morphologies and supramolecular organizations, which resulted in agreement with the outcomes reported in the previous XRD and ssNMR investigations.

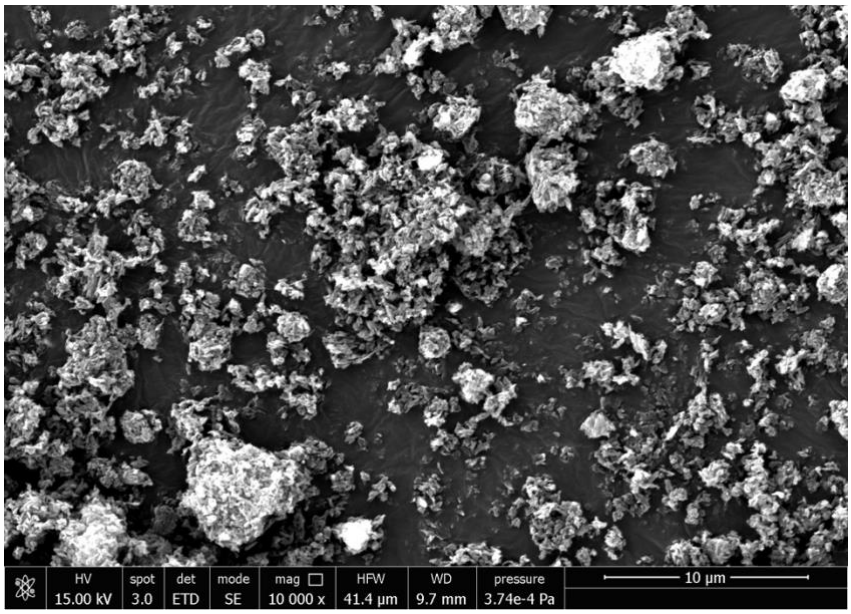


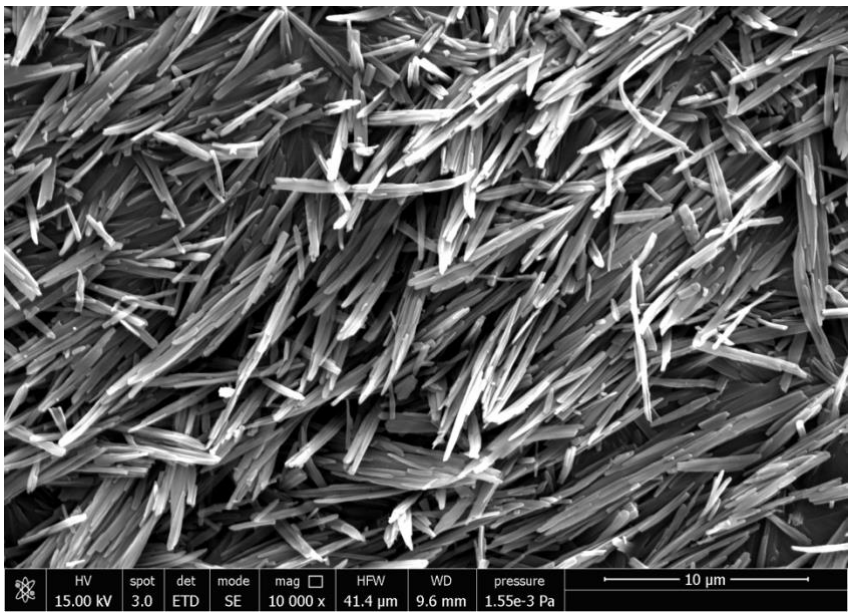


Figure 4. a) SEM micrographs of P-black C and b) P-black S

Notably, P-black C appeared as an irregular distribution of assemblies made by very short elongated pigment aggregates with a maximum length of about 1.5 μm (Figure S2a). Conversely, a more compact, regular and uniform distribution of rod-like structures with a long-range order emerged from the analysis of the synthetic form of the pigment, whose monodimesional aggregates exceeded 6-7 μm in length

(Figure S2b). These longer and compact assemblies of P-black S could possibly favor the formation of a homogeneous layer of pigment with enhanced NIR reflective characteristics.

*NIR reflective features and solar reflectance*

Acrylic water dispersions containing 5 wt.% and 10 wt.% of P-black C and P-black S pigments were then coated at a thickness of 75 µm over the white and black portions of Leneta® checkboards. UV-VIS-NIR reflectance spectra were recorded up to 2500 nm for all the samples. Reflectances of the white substrates (Figure 5a) show a clear feature depending on the P-black content and optical characteristics.[41]

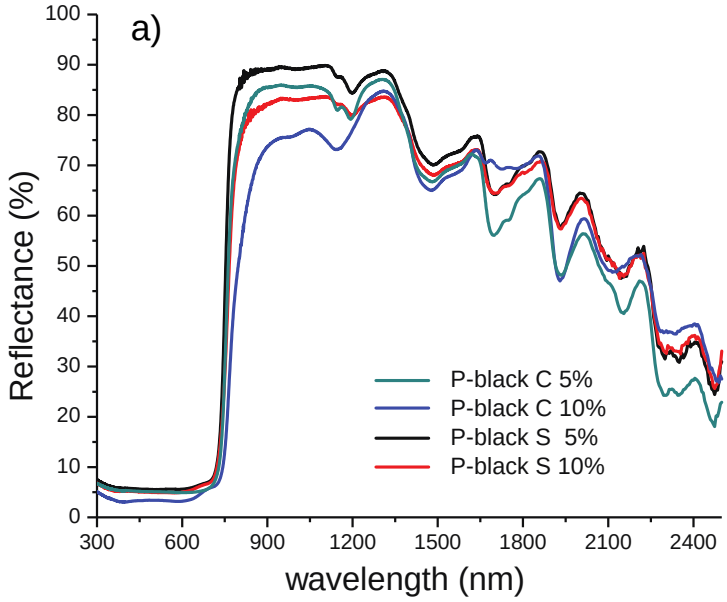

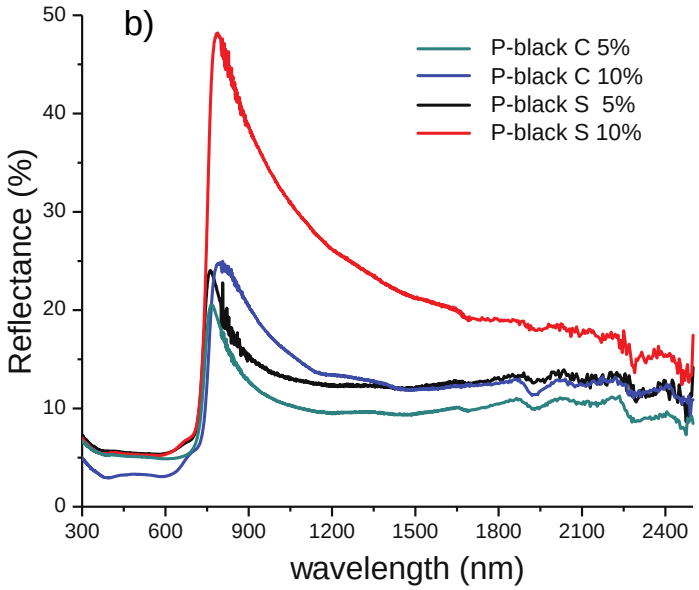


**Figure 5.** UV-VIS-NIR reflectance spectra of P-black acrylic coatings (thickness of = 75 μm) on white a) and black b) substrates.

Notably, reflectance values are close to zero in the visible region up to 750 nm for all the samples due to the strong absorption provided by the pigment stacked structures.[29] Conversely, the pigments appear NIR transparent with reflectances higher than 80% at 1300 nm and similar to those of the bare acrylic coating (Figure S3, blue curve). It is worth noting that the NIR transparency results more evident for the synthesized P-black S, since the coating based on the commercial P-black C displays stronger absorptions for all the respective concentration.

Reflectance spectra of the coated black substrate revealed the NIR reflective features of P-black pigments (Figure 5b). A reflectance peak at about 900 nm flanked by a long tail is recorded for all the investigated coatings up to 2500 nm and above the contribution of the bare coating (Figure S3, red curve). Notably, the commercial P-black C pigment provided maximum reflectance values of about 25 % even at the highest pigment content of 10 wt.%, whereas this performance is already matched by the 5 wt.% of the P-black S. The remarkable NIR reflective features of the synthetic P-black dispersion were confirmed by the coating layer containing the 10 wt.% of the pigment. Reflectance maximum of about 50% and values

above 25% in the 800-1200 nm wavelength interval was recorded, and appeared particularly relevant since about 50% of the NIR energy and the 25% of the total energy of the solar spectrum fall in such wavelength interval.[5] These findings, combined with the XRD and ssNMR investigations, indicate that the higher structural order and degree of crystallinity of the P-black S pigment result in acrylic coatings with more pronounced NIR reflectivity. This enhanced contribution was also possibly favored by the regular elongated and compact structure of the P-black S assemblies as determined by SEM micrographs. The greater NIR reflective features of the acrylic coatings based on P-black S were also confirmed in terms of the solar reflectance (SR) that was measured according over the black substrates and in agreement with the ASTM G173-03 (Table 1).[29]

**Table 1.** SR values of the P-black coatings of a thickness of 75 μm on black substrates and average temperatures of the back side of the coated substrate measured after irradiation for 15 min with a solar simulator.

| Entry | Concentration (wt.%) | SR (%) | Average temperature (°C) |
|---|---|---|---|
| Black substrate | - | 5.0 | 42.3 |
| P-black C | 5 | 8.7 | 40.4 |
| | 10 | 9.9 | 40.0 |
| P-black S | 5 | 10.4 | 39.6 |
| | 10 | 18.2 | 38.5 |

SR near 5-6 % are generally measured on black or highly absorbing dark substrates.[49] Covering this substrate with the P-black C dispersion, SR values increased up to 10% at the highest pigment content of 10 wt.%, that is in agreement with literature data and the NIR reflective features of the PBI derivative.[42] Noteworthy, the use of synthetic P-black S with higher crystalline content provided a remarkable increase of the SR up to maximum values of 18.2%, i.e. about twice the contribution of the corresponding P-black C and consistent with the pronounced NIR reflection in the 800-1200 nm wavelength interval. The cooling effect conferred by the NIR reflective features of P-black dispersions were also evaluated in terms of the average temperature of the internal side of the coated substrates (Table

1) after the illumination for 15 min with a solar simulator. A progressive decreasing of the internal temperature was recorded for all the samples as a function of P-black pigment concentration. These characteristics were particularly evident for the black substrates coated by the synthetic P-black S derivative, whose 5 wt.% content exceeded the cooling effect provided by the 10 wt.% content of the corresponding P-black C. The effect provided by P-black S on the cooling characteristics of the acrylic coating was visibly clear by inspecting the plot of Figure 5. It is worth noting that temperature decreasing of about 4-5 °C was recorded at the highest content of P-black S, in agreement with the significant 18.2% of solar reflectance and attributed to the superior scattering features of the more crystalline assemblies of the synthetic P-black pigment.

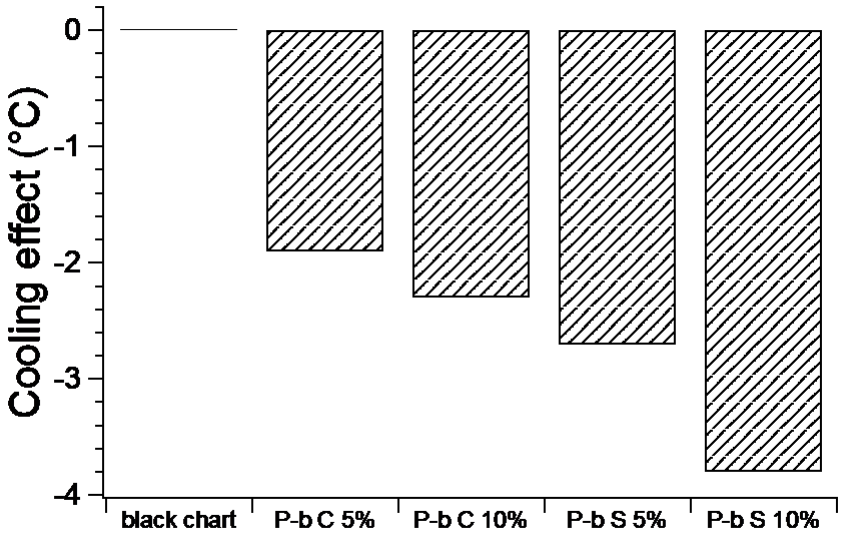


**Figure 5.** Cooling effect of the P-black (P-b) coatings of a thickness of 75 μm on black substrates. The average temperature of the internal side of the coated substrates was measured after irradiation for 15 min with a solar simulator.

## Conclusions

This work demonstrated the beneficial contribution of the crystallinity degree and structural order of supramolecular assemblies of the perylene derivative P-black on the NIR reflective and cooling

characteristics of acrylic coatings of black substrates. Notably, P-black provided NIR transparent and NIR reflective features that were particularly enhanced when the synthetic pigment form was utilized. XRD evidenced an increase of crystallinity (from 20 to 48%), mean crystallite size (from 21.7 to 39.1 nm) and structural order on passing from P-black C to P-black S, in agreement with an increase of structural and dynamic order found by SSNMR and confirmed by SEM analysis. In particular, $^{13}C$ signals ascribable to a fraction of P-black molecules characterized by a partial dynamic disorder, probably located in proximity to the edges of the stacked structures, were observed in the $^{13}C$ CP/MAS spectrum of P-black C, while it was not detectable for the synthetic P-black S pigment. All these features favored the emersion of more effective scattering phenomena within the acrylic coatings and boosted the NIR reflection over black surfaces in the 800-1200 nm wavelength interval, i.e. providing maximum SR of 18.2% at the highest content (10 wt.%) of P-black S. This considerable data yielded a maximum cooling effect of about 4 °C of the internal side of the coated surface, i.e. about 1.5 °C larger than that provided by the commercial pigment.

**Acknowledgements**

This work was supported by the Tuscany region POR FESR 2014-2020 COOLSUN - New NIR-reflective “cool” organic pigments. CISUP - Centre for Instrumentation Sharing - University of Pisa is kindly acknowledged for SEM measurements.

**References**

[1] Nowak-Król A, Würthner F. Progress in the synthesis of perylene bisimide dyes. Organic Chemistry Frontiers. 2019;6(8):1272-318.
[2] Görl D, Zhang X, Würthner F. Molecular assemblies of perylene bisimide dyes in water. Angewandte Chemie - International Edition. 2012;51(26):6328-48.
[3] Würthner F, Kaiser TE, Saha-Möller CR. J-aggregates: From serendipitous discovery to supramolecular engineering of functional dye materials. Angewandte Chemie - International Edition. 2011;50(15):3376-410.

[4] Chen Z, Lohr A, Saha-Möller CR, Würthner F. Self-assembled π-stacks of functional dyes in solution: Structural and thermodynamic features. Chemical Society Reviews. 2009;38(2):564-84.
[5] Kaur B, Quazi N, Ivanov I, Bhattacharya SN. Near-infrared reflective properties of perylene derivatives. Dyes Pigm. 2012;92(3):1108-13.
[6] Mazhar M, Abdouss M, Gharanjig K, Teimuri-Mofrad R. Synthesis, characterization and near infrared properties of perylenebisimide derivatives. Prog Org Coat. 2016;101:297-304.
[7] Würthner F. Perylene bisimide dyes as versatile building blocks for functional supramolecular architectures. Chemical Communications. 2004(14):1564-79.
[8] Carlotti M, Gullo G, Battisti A, Martini F, Borsacchi S, Geppi M, et al. Thermochromic polyethylene films doped with perylene chromophores: Experimental evidence and methods for characterization of their phase behaviour. Polymer Chemistry. 2015;6(21):4003-12.
[9] Donati F, Pucci A, Cappelli C, Mennucci B, Ruggeri G. Modulation of the optical response of polyethylene films containing luminescent perylene chromophores. Journal of Physical Chemistry B. 2008;112(12):3668-79.
[10] Raj MR, Margabandu R, Mangalaraja RV, Anandan S. Influence of imide-substituents on the H-type aggregates of perylene diimides bearing cetyloxy side-chains at bay positions. Soft Matter. 2017;13(48):9179-91.
[11] Liu X, Wang KR, Rong RX, Liu MH, Wang Q, Li XL. Host-guest controlled assembly and recognition of perylene bisimide-based glycocluster with cyclodextrin. Dyes and Pigments. 2020;174.
[12] Li S, Long T, Wang Y, Yang X. Self-assembly, protonation-dependent morphology, and photophysical properties of perylene bisimide with tertiary amine groups. Dyes and Pigments. 2020;173.
[13] Wang Z, Wang G, Chang X, Liu K, Qi Y, Shang C, et al. A Perylene Bisimide-Contained Molecular Dyad with High-Efficient Charge Separation: Switchability, Tunability, and Applicability in Moisture Detection. Advanced Functional Materials. 2019;29(44).
[14] Tian Z, Guo Y, Li J, Li C, Li W. Benzodithiophene-Fused Perylene Bisimides as Electron Acceptors for Non-Fullerene Organic Solar Cells with High Open-Circuit Voltage. ChemPhysChem. 2019;20(20):2696-701.
[15] Gupta RK, Sudhakar AA. Perylene-Based Liquid Crystals as Materials for Organic Electronics Applications. Langmuir. 2019;35(7):2455-79.
[16] Schiphorst Jt, Kendhale AM, Debije MG, Menelaou C, Herz LM, Schenning APHJ. Dichroic Perylene Bisimide Triad Displaying Energy Transfer in Switchable Luminescent Solar Concentrators. Chemistry of Materials. 2014;26(13):3876-8.
[17] Gutierrez GD, Coropceanu I, Bawendi MG, Swager TM. A Low Reabsorbing Luminescent Solar Concentrator Employing π-Conjugated Polymers. Advanced Materials. 2016;28(3):497-501.
[18] Iasilli G, Francischello R, Lova P, Silvano S, Surace A, Pesce G, et al. Luminescent solar concentrators: boosted optical efficiency by polymer dielectric mirrors. Mat Chem Front. 2019;3(3):429-36.
[19] Geervliet TA, Gavrila I, Iasilli G, Picchioni F, Pucci A. Luminescent Solar Concentrators Based on Renewable Polyester Matrices. Chem-Asian J. 2019;14(6):877-83.
[20] Mori R, Iasilli G, Lessi M, Muñoz-García AB, Pavone M, Bellina F, et al. Luminescent solar concentrators based on PMMA films obtained from a red-emitting ATRP initiator. Polymer Chemistry. 2018;9(10):1168-77.
[21] Carlotti M, Ruggeri G, Bellina F, Pucci A. Enhancing optical efficiency of thin-film luminescent solar concentrators by combining energy transfer and stacked design. Journal of Luminescence. 2016;171:215-20.
[22] Carlotti M, Fanizza E, Panniello A, Pucci A. A fast and effective procedure for the optical efficiency determination of luminescent solar concentrators. Solar Energy. 2015;119:452-60.

[23] Matussek M, Filapek M, Gancarz P, Krompiec S, Grzegorz Małecki J, Kotowicz S, et al. Synthesis and photophysical properties of new perylene bisimide derivatives for application as emitting materials in OLEDs. Dyes and Pigments. 2018;159:590-9.
[24] Pucci A. Mechanochromic fluorescent polymers with aggregation-induced emission features. Sensors (Switzerland). 2019;19(22).
[25] Minei P, Pucci A. Fluorescent vapochromism in synthetic polymers. Polymer International. 2016;65(6):609-20.
[26] Ciardelli F, Ruggeri G, Pucci A. Dye-containing polymers: Methods for preparation of mechanochromic materials. Chemical Society Reviews. 2013;42(3):857-70.
[27] Pucci A, Ruggeri G. Mechanochromic polymer blends. Journal of Materials Chemistry. 2011;21(23):8282-91.
[28] Pucci A, Bizzarri R, Ruggeri G. Polymer composites with smart optical properties. Soft Matter. 2011;7(8):3689-700.
[29] Minei P, Lessi M, Contiero L, Borsacchi S, Martini F, Ruggeri G, et al. Boosting the NIR reflective properties of perylene organic coatings with thermoplastic hollow microspheres: Optical and structural properties by a multi-technique approach. Solar Energy. 2020;198:689-95.
[30] Mazhar M, Abdouss M, Gharanjig K, Teimuri-Mofrad R, Zargaran M. Effects of isomerism on near infrared properties of perylene bisimide derivatives. Journal of Coatings Technology and Research. 2017;14(1):207-14.
[31] Qu J, N Zhang Z, D Shi W, X Zhang Y, Xue T, Zhang X, et al. The Optical Properties of Black Coatings and Their Estimated Cooling Effect and Cooling Energy Savings Potential2014.
[32] Kaur B, Bhattacharya SN, Henry DJ. Interpreting the near-infrared reflectance of a series of perylene pigments. Dyes and Pigments. 2013;99(2):502-11.
[33] Jose S, Joshy D, Narendranath SB, Periyat P. Recent advances in infrared reflective inorganic pigments. Solar Energy Materials and Solar Cells. 2019;194:7-27.
[34] Synnefa A, Santamouris M, Apostolakis K. On the development, optical properties and thermal performance of cool colored coatings for the urban environment. Solar Energy. 2007;81(4):488-97.
[35] Levinson R, Berdahl P, Akbari H. Solar spectral optical properties of pigments—Part I: model for deriving scattering and absorption coefficients from transmittance and reflectance measurements. Solar Energy Materials and Solar Cells. 2005;89(4):319-49.
[36] Raj AKV, Rao PP, Sreena TS, Thara TRA. Pigmentary colors from yellow to red in Bi2Ce2O7 by rare earth ion substitutions as possible high NIR reflecting pigments. Dyes and Pigments. 2019;160:177-87.
[37] Ianoş R, Muntean E, Lazău R, Băbuță R, Moacă E-A, Păcurariu C, et al. One-step synthesis of near-infrared reflective brown pigments based on iron-doped lanthanum aluminate, LaAl1-xFexO3. Dyes and Pigments. 2018;152:105-11.
[38] Schildhammer D, Fuhrmann G, Petschnig L, Weinberger N, Schottenberger H, Huppertz H. Synthesis and characterization of a new high NIR reflective ytterbium molybdenum oxide and related doped pigments. Dyes and Pigments. 2017;138:90-9.
[39] Mahmoudi Meymand F, Mazhar M, Abdouss M. Investigation of substituent effect on cool activity of perylene bisimide pigments. J Coat Technol Res. 2019;16(2):439-47.
[40] Muniz-Miranda F, Minei P, Contiero L, Labat F, Ciofini I, Adamo C, et al. Aggregation Effects on Pigment Coatings: Pigment Red 179 as a Case Study. ACS Omega. 2019;4(23):20315-23.
[41] Mazhar M, Abdouss M, Gharanjig K, Teimuri-Mofrad R. Synthesis, characterization and near infra-red properties of perylenebisimide derivatives. Progress in Organic Coatings. 2016;101:297-304.
[42] BASF. Paint it cool! Pigments for solar heat management in paints.
[43] BASF. NN' Para methoxy benzyl perylene-3,4,9,10-tetracarboxylic acid diimide. US 4,450,273 ed1984.

[44] Zanchetta G, Bini M, Giaccio B, Manganelli G, Benocci A, Regattieri E, et al. Middle Pleistocene (MIS 14) environmental conditions in the central Mediterranean derived from terrestrial molluscs and carbonate stable isotopes from Sulmona Basin (Italy). Palaeogeography, Palaeoclimatology, Palaeoecology. 2017;485:236-46.
[45] Alexander L, Klug HP. Determination of Crystallite Size with the X-Ray Spectrometer. Journal of Applied Physics. 1950;21(2):137-42.
[46] Carignani E, Borsacchi S, Geppi M. Dynamics by Solid-State NMR: Detailed Study of Ibuprofen Na Salt and Comparison with Ibuprofen. The Journal of Physical Chemistry A. 2011;115(32):8783-90.
[47] Martini F, Borsacchi S, Spera S, Carbonera C, Cominetti A, Geppi M. P3HT/PCBM Photoactive Materials for Solar Cells: Morphology and Dynamics by Means of Solid-State NMR. The Journal of Physical Chemistry C. 2013;117(1):131-9.
[48] Sottile M, Tomei G, Borsacchi S, Martini F, Geppi M, Ruggeri G, et al. Epoxy resin doped with Coumarin 6: Example of accessible luminescent collectors. European Polymer Journal. 2017;89:23-33.
[49] Levinson R, Berdahl P, Akbari H. Solar spectral optical properties of pigments—Part II: survey of common colorants. Solar Energy Materials and Solar Cells. 2005;89(4):351-89.

**Supporting information** of the manuscript "Structural order and NIR reflective properties of perylene bisimide pigments: experimental evidences from a combined multi-technique study" by *Francesca Martini,[1,2,3] Pierpaolo Minei,[1] Marco Lessi,[1] Luca Contiero,[4] Silvia Borsacchi,[2,5] Giacomo Ruggeri,[1,2] Marco Geppi,[1,2,3] Fabio Bellina,[1,2,3] Andrea Pucci[1,2,3,*]*

[1]Dipartimento di Chimica e Chimica Industriale, Università di Pisa, Via Giuseppe Moruzzi 13, 56124 Pisa, Italy
[2]INSTM, UdR Pisa, Via Giuseppe Moruzzi 13, 56124 Pisa, Italy
[3]CISUP, Centro per l'Integrazione della Strumentazione dell'Università di Pisa, Lungarno Pacinotti 43, Pisa
[4]Cromology Italia S.P.A. Via 4 Novembre 4, 55016 Porcari, Lucca, Italy
[5]Istituto di Chimica dei Composti Organo Metallici (ICCOM), Consiglio Nazionale delle Ricerche, SS Pisa, Via G. Moruzzi 1, 56124 Pisa, Italy

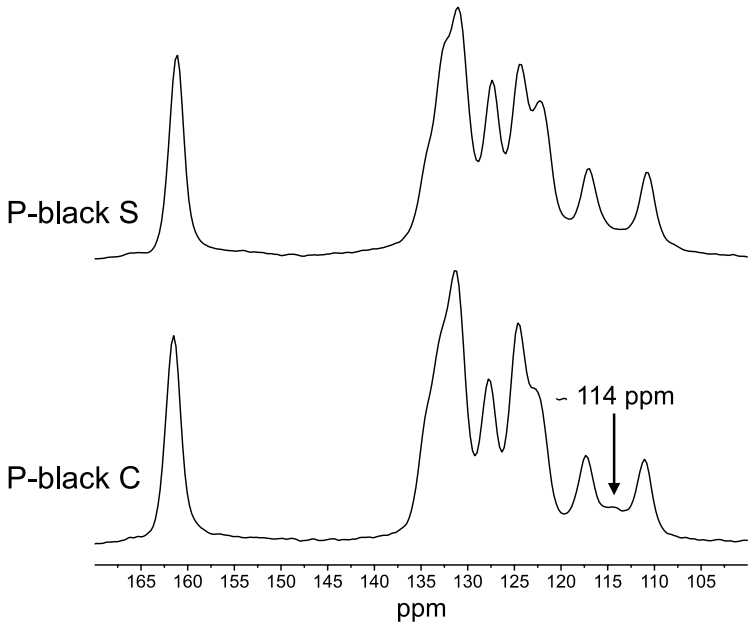


**Figure S1.** Expansion of the aromatic spectral region of the $^{13}C$ CP/MAS spectra of P-black C and P-black S. The peak at 114 ppm, discussed in the main text, is clearly visible only in the spectrum of P-black C and is indicated by an arrow.

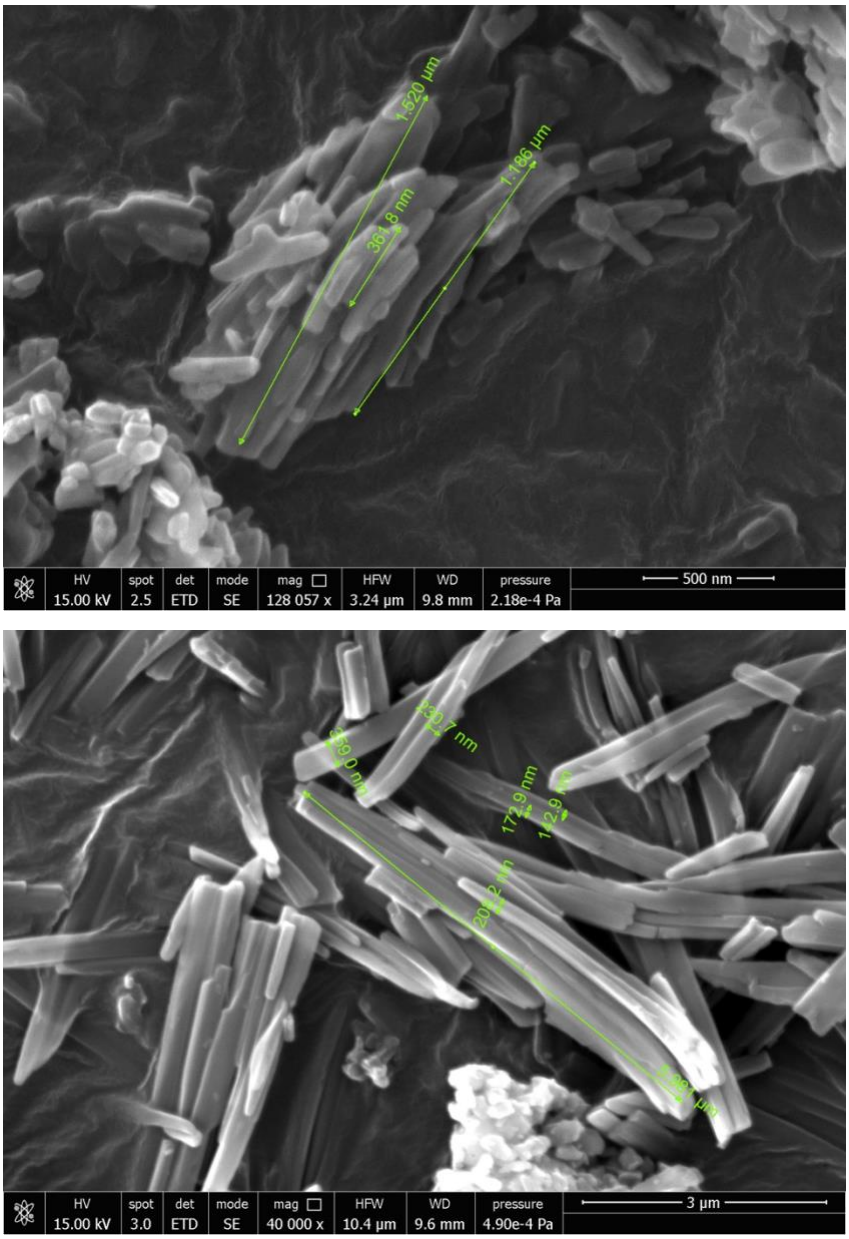


**Figure S2.** a) SEM micrographs of P-black C and b) P-black S at high magnifications

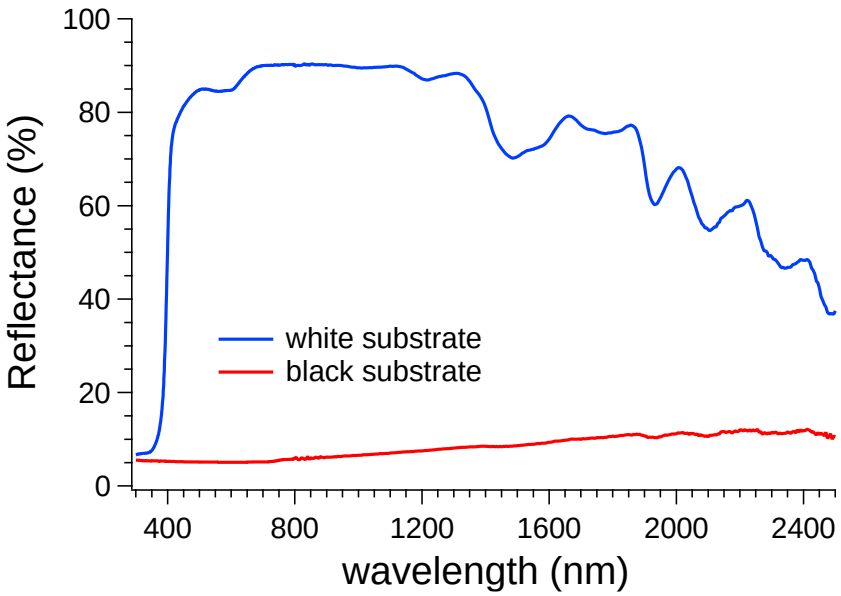


**Figure S3.** UV-VIS-NIR reflectance spectra of the neat acrylic coating without P-black over the white (blue curve) and black (red curve) portion of Leneta® checkerboard charts

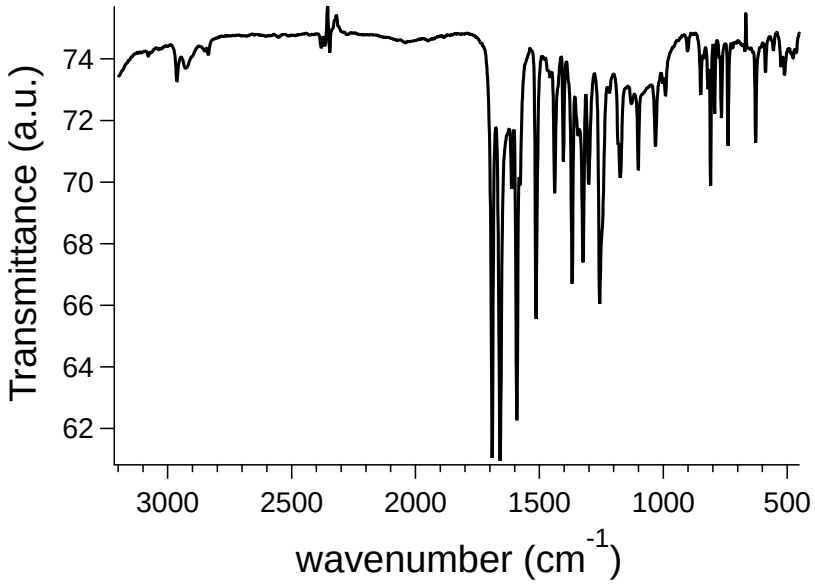


**Figure S4.** FTIR spectrum of P-black S

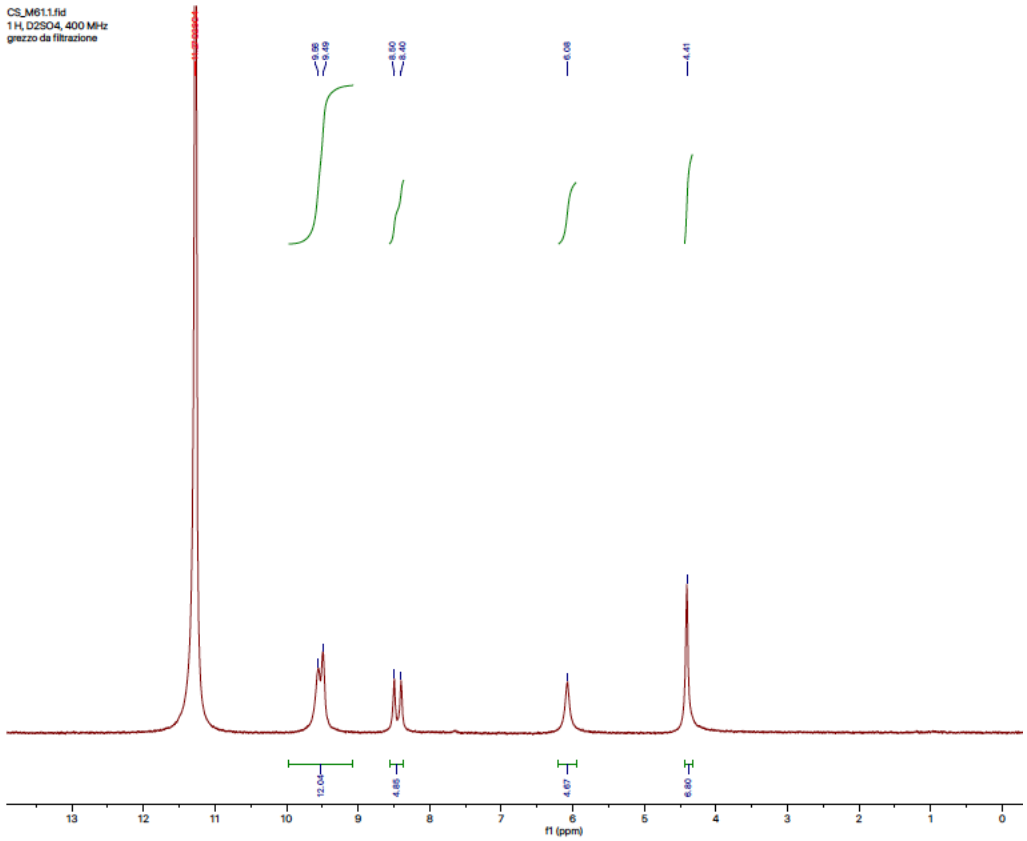


**Figure S5.** $^{1}H$ NMR spectrum of P-black S in $D_2SO_4$